Turk J Chem
26 (2002) , 915 – 924.

Anodic Behavior of Tungsten in H_3PO_4-K_2SO_4-H_2SO_4/KOH Solutions

Mustafa ANIK
Metallurgy Institute, Osmangazi University,
26480, Eskişehir-TURKEY
e-mail: manik@ogu.edu.tr

Received 28.01.2002

Potentiodynamic and potentiostatic polarizations were used to study the effect of pH on the anodic reaction characteristics of tungsten (W) in a very broad pH range (0.4-13). The open circuit potential was observed to decrease with a constant slope of 58 mV/pH, as pH increased. The oxide phase of W showed typical amphoteric surface behavior in the acidic regime. The oxide dissolution went through a minimum at pH 2.5, which was identified as the point of zero charge (pzc) of W–oxide. The oxide dissolution below the pzc was H^+-assisted and above the pzc was OH^--assisted. At around the pzc the main dissolution pathway was H_2O-assisted dissolution. In basic solutions, in the pH range 7 to 10.5, the hydrated oxide phase dissolution was pH independent. In very basic solutions (above pH 10.5), the dissolution rate of W was observed to increase as pH increased.

Introduction

The electrochemical behaviors of tungsten (W) and W-oxides have attracted great technological interest for a long time[1−29]. The anodic characteristics of W in a large pH range in H_3PO_4-KNO_3 solutions were reported previously[30]. Potassium nitrate (KNO_3), however, is not the most inert supporting electrolyte to use in electrochemical systems due to the possible redox reactions of NO_3^- ions especially in acidic solutions[31]. In order to eliminate any influence on the results from NO_3^- redox reactions, K_2SO_4 is used as a supporting electrolyte in this study and the anodic behavior of W is re-examined by conducting potentiodynamic and potentiostatic polarization experiments in the pH range 0.4 to 13. The ionic strength of the solution is kept constant and the data are collected especially in the pH levels where H_3PO_4 acts as a good pH buffer (2 ± 1, 7 ± 1, 12 ± 1). The results obtained from this investigation, as in the previous publication[30], are compared and combined with those reported in the literature to support our attempts to develop a unified theory for W anodic reactions.

Materials and Methods

A tungsten (W) rod, 0.4 cm in diameter (99.99% purity) was obtained from Aldrich. H_3PO_4, K_2SO_4 and KOH were purchased from Merck and H_2SO_4 was purchased from PRS Ponreac. All aqueous solutions,

prepared from distilled water, were bubbled with Ar gas. All test solutions were buffered using 0.1 M H_3PO_4 and pH was adjusted with H_2SO_4 or KOH. The ionic strength ($I = \frac{1}{2}\Sigma\ c\ z^2$, where c is the concentration (molarity) and z is the charge) of 2 M was kept constant by the use of K_2SO_4 for all test solutions. The compositions of the test solutions used in this investigation are tabulated in the Table.

The W electrode used in the electrochemical experiments was placed in a small mould, which was then filled with resin. After the resin had hardened, the electrode was abraded by 500, 600, 800 and 1200 grit grinding papers. The exposed electrode surface (geometric area of 0.126 cm^2) was polished with 1 μm diamond paste prior to each experiment. The polished electrode was rinsed with acetone and the test solution. Special care was taken to keep the time as short as possible between polishing the specimen and inserting it into the test cell.

Table. The compositions of the test solutions used in this study. The concentrations of the chemicals are in molarity.

Sol. No	H_3PO_4	H_2SO_4	KOH	K_2SO_4	pH
1	0.100	0.467	0.000	0.500	≈ 0.4
2	0.100	0.200	0.000	0.600	1.1
3	0.100	0.000	0.000	0.650	2.1
4	0.100	0.000	0.030	0.457	2.4
5	0.100	0.000	0.055	0.638	2.6
6	0.100	0.000	0.070	0.631	2.9
7	0.100	0.000	0.090	0.621	3.6
8	0.100	0.000	0.096	0.618	4.5
9	0.100	0.000	0.120	0.609	5.7
10	0.100	0.000	0.150	0.593	6.8
11	0.100	0.000	0.200	0.561	7.5
12	0.100	0.000	0.223	0.530	8.6
13	0.100	0.000	0.240	0.520	10.1
14	0.100	0.000	0.290	0.501	11.3
15	0.100	0.000	0.350	0.453	12.5
16	0.100	0.000	0.500	0.380	13.0

A standard three-electrode system consisting of a working electrode, a counter electrode (carbon rod, 0.6 cm in diameter), and a reference electrode (saturated calomel electrode) was used. A model PC4/300 mA Potentiostat/Galvanostat (Gamry Inst.) controlled by DC105 DC Corrosion Software (Gamry Inst.) was used in the electrochemical measurements. All experiments were performed in a 800 ml glass cell.

Open circuit potential (Eoc) curves were obtained by holding the electrode at Eoc for about 20 min, which was enough time to get the steady-state potential values. Potentiodynamic polarization curves were generated by sweeping the potential from the potential 100 mV less than Eoc to 1200 mV at a scan rate of 1 mVs^{-1}. Potentiostatic polarizations were carried out by holding the electrode potential constant at 1000 mV for 20 min. Unless indicated otherwise, all potentials refer to the saturated calomel electrode, SCE (SCE, 241 mV vs. SHE). All experiments were conducted at laboratory temperature (20 ± 1°C).

The stability diagrams for the W–H_2O system were generated with the DIAGRAM software[32].

Results and Discussions

Solution chemistry of the W–H_2O system

The activity of total dissolved W is fixed at a constant value of 10^{-4} in the Eh–pH diagrams presented in Figures 1 and 2. The dashed lines in the diagrams represent the limits of stability of water. Figure 1 shows that in the narrow potential region WO_2(s) and W_2O_5(s) are stable W–oxides in the pH ranges 0–7 and 0–5, respectively. WO_3(s), however, is stable only below pH 2 throughout the oxidizing conditions. In the pH range 2 to 5, the oxidizing conditions favor the formation of polytungstate $W_{12}O_{39}^{6-}$(aq). The increase in the dissolved metal concentration in acidic solutions also results in formation of different kinds of polytungstates[30]. If the formation of tungstic acid ($WO_3.H_2O$(s) = H_2WO_4(s)) is considered[15], as shown in the metastable Eh–pH diagram in Figure 2, it becomes the only stable W–oxide form under all oxidizing conditions up to pH 6. In the basic conditions, in both stability diagrams in Figures 1 and 2, WO_4^{2-} is the predominant species in solution. Therefore, WO_4^{2-} can be expected as a product of both active W metal and W–oxide dissolutions in basic solutions.

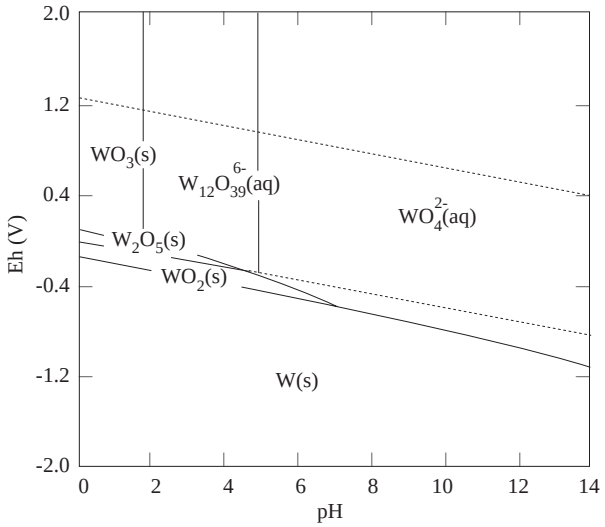

Figure 1. Eh-pH diagram for the W-H_2O system; [W] = 10^{-4}.

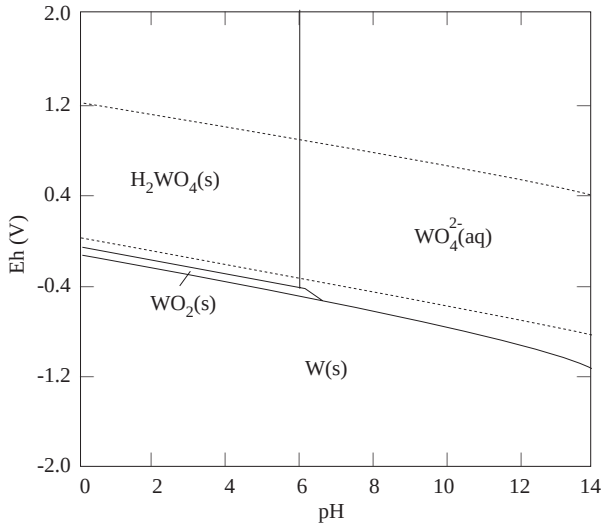

Figure 2. Metastable Eh-pH diagram for the W-H_2O system; [W] = 10^{-4}.

Open circuit potentials

The open circuit potential (Eoc) data obtained at various pH values are shown by generating a pH vs. Eoc curve as in Figure 3 (note that the potentials refer to SHE). The slope of the line (dEoc/dpH) is 58 mV in Figure 3. This value indicates a 1:1 ratio of H^+ to electrons for the reaction that controls Eoc. Voltage values in the acidic regime in Figure 3 correspond to the neighborhood of the W_2O_5(s)/WO_3(s) boundary line in Figure 1. Therefore the Eoc of W in acidic solutions can be assumed to be controlled by the following reaction[30]:

$$1/2W_2O_5(s) + 1/2H_2O \rightarrow WO_3(s) + H^+ + e^- \quad (1)$$

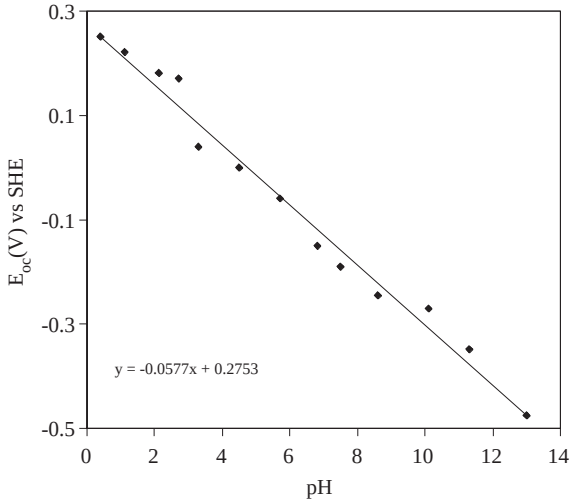

Figure 3. The effect of pH on the open circuit potential.

According to the reported results[8] the Eoc controlling reaction in basic solutions, however, may be like the form in Reaction 2:

$$WO_2(s) + OH^- \rightarrow WO_3H(s) + e^- \tag{2}$$

Reaction 2 must be followed by faster reactions like the ones in Equations 3 and 4, since the dissolution rate of W–oxides is quite high in basic solutions[8,30].

$$WO_3H(s) + OH^- = WO_3(s) + H_2O + e^- \tag{3}$$

$$WO_3(s) + 2OH^- = WO_4^{2-}(aq) + H_2O \tag{4}$$

The scatter in Eoc data at around pH 3 and in the pH range 8 to 10 in Figure 3 may be best understood after the discussions in the subsequent sections.

Potentiodynamic anodic polarization of W

The effect of pH on the anodic polarization behavior of W is given in Figure 4. The open circuit potential shifts to less noble potentials as pH increases as explained in detail in the previous section. The anodic currents of W, however, show different dependence on the pH change. Initially, at all pH values the anodic current increases with the applied anodic potential to a certain value. This increase results from oxidation of the lower oxidation state W–oxide to the higher oxidation state W–oxide as in Reactions 1 and 2. At pH 0.4 anodic current levels off when it reaches 10^{-5} Acm^{-2}. The absence of reduction in the anodic current after leveling off upon application of more anodic potential suggests that the oxide layer formed on W at this pH level is not quite protective[7,11,12]. As pH increases to pH 2.6, the anodic current of W decreases. A further reduction in the anodic currents at around 700 mV at pH 1.1 and especially at pH 2.6 suggests the presence of a protective oxide layer on the metallic W at these pH levels. In fact, the decrease in the anodic currents of W as pH increases can be explained by the formation of a more protective oxide layer. Above pH 2.6, as pH increases the anodic currents of W also increases. This change in the pH dependence of the W reaction can be explained by the change in the mechanism of the rate controlling anodic reaction, as will be made clearer in the forthcoming discussions. The reduction in anodic current at 700 mV is also apparent

at pH 6.8 and even at pH 11.3. Therefore, it can be assumed that although it is not observed in the stability diagrams in Figures 1 and 2 the oxide layer is also present on the metallic W in weakly alkaline solutions. In strongly alkaline solutions (pH 13), however, there is a well-defined limiting anodic current, the presence of which will also be discussed in the next sections.

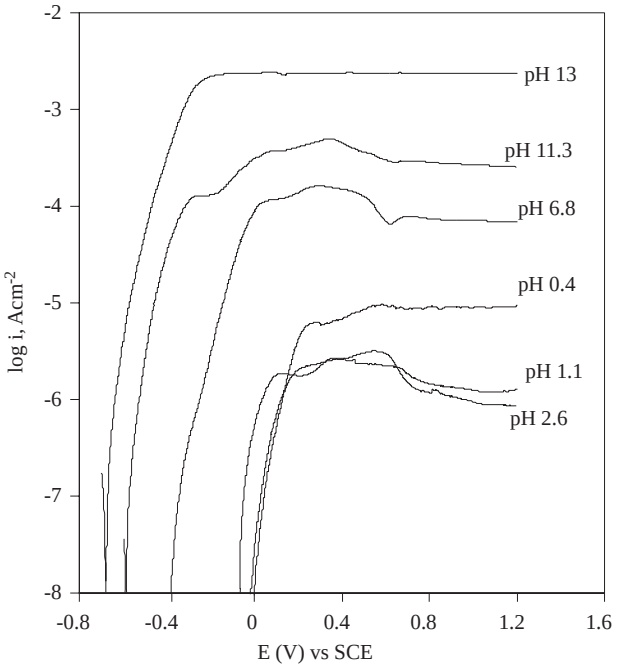

Figure 4. Effect of the pH on the potentiodynamic anodic polarization behavior of W; scan rate = 1 mVs^{-1}.

Although potentiodynamic polarizations give very useful information about W anodic reactions in a very broad potential range, the potentiostatic anodic currents will be very helpful in developing the reaction mechanisms.

Potentiostatic anodic polarization of W

As evidenced in the open circuit potential section, the Eoc of W shifts to less noble potentials as pH increases with a constant slope of 58 mV/pH. Therefore, a high anodic potential value must be selected in order to obtain constant potential pH dependence of the anodic current in a wide pH range. For this purpose, the potentiostatic anodic current curves are generated with the application of constant 1 V anodic potential for all pHs.

Some of the selected steady-state anodic currents obtained at 1 V are shown in Figure 5a for pH 0.4, 1.1 and 2.6, in Figure 5b for pH 0.4 and 6.8, and in Figure 5c for pH 6.8, 10.1 and 13. Upon application of 1 V anodic potential, the anodic current first decreases for a few seconds and then starts to increase, and then levels off by reaching a steady-state value at pH 0.4 in Figure 5a. This behavior suggests that with the application of anodic potential, the protective oxide layer forms on W surface; a few seconds later, however, this oxide layer dissolves at a relatively high rate. The increase in pH causes anodic current to decrease in Figure 5a. Although there is no tendency of increase in the anodic current over time at pH 2.6, there is a slight increase in current at pH 1.1 just after application of the potential for about 300 s. The increase in pH results in an increase in anodic currents in Figures 5b and 5c, in contrast to the trend in Figure 5a. This

change in pH dependence suggests a change in the mechanism of the rate controlling the anodic reaction in acidic solutions. The sharp decrease in current is followed by a sharp increase in just a few seconds, and then leveling off is apparent at pH 6.8 just as in the case at pH 0.4 in Figure 5b. Obviously, the dissolution rate of the oxide at pH 6.8 is much higher than that of the oxide at pH 0.4. Despite only about a two fold increase in the steady-state current with the increase at pH levels from 6.8 to 10.1, the increase in the steady-state anodic current is about 15-fold with the increase at pH levels from 10.1 to 13 in Figure 5c. Once again this different pH dependence of the steady-state anodic current suggests the validity of different mechanisms for the rate controlling reactions at different pH levels in basic solutions.

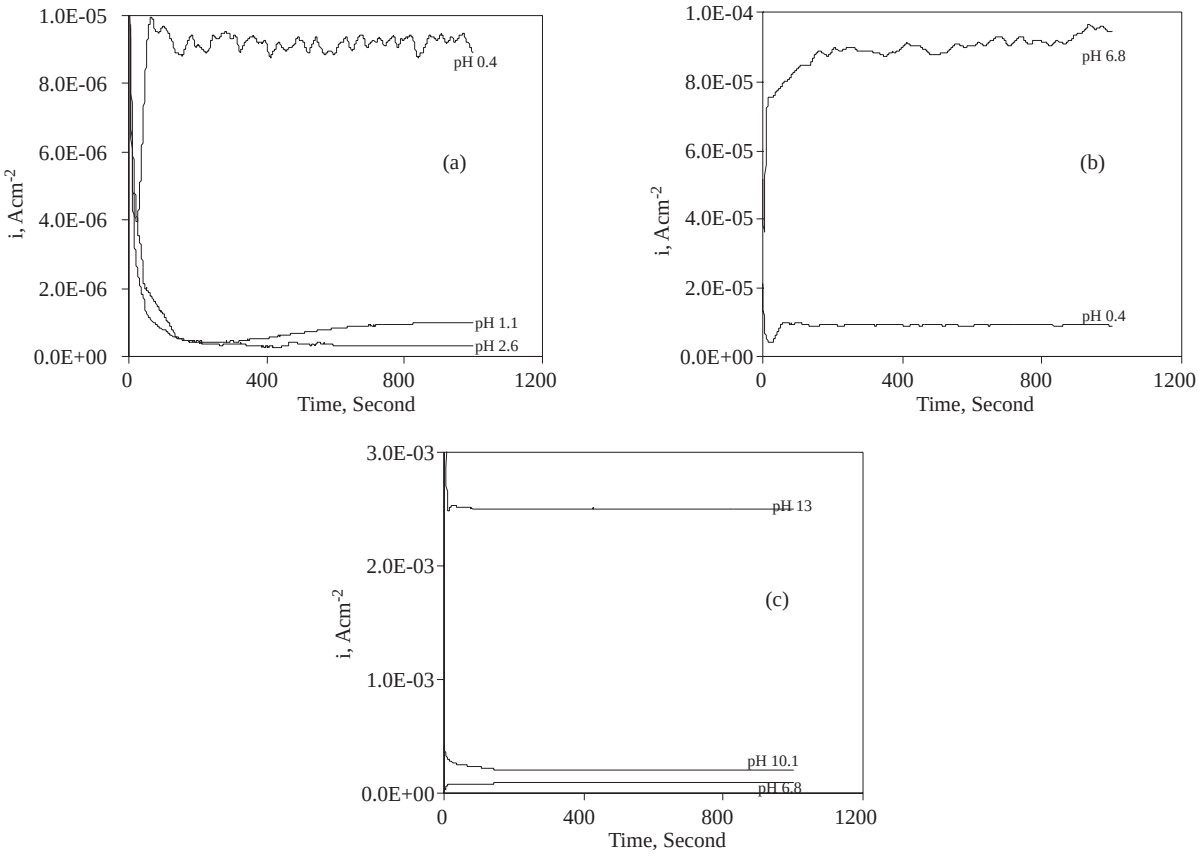

Figure 5. Effect of pH on the steady-state currents obtained at constant 1 V: (a) pH 0.4, 1.1, 2.6, (b) pH 0.4, 6.8, (c) pH 6.8, 10.1, 13.

The trends in Figures 5a, 5b and 5c can be shown more clearly by generating the log i vs. pH plot as in Figure 6. All the steady-state current values obtained in this study (see the Table) are not given in Figures 5a, 5b or 5c for a clear representation of the results. However, all the steady-state current data gathered are used to generate the plot in Figure 6. This figure shows the limits of distinct pH regions where the mechanisms of the rate controlling anodic reactions are different.

Mechanisms of W anodic reactions

As noted before, Eoc is controlled by the reaction in Equation 1 in acidic solutions. This reaction also accounts for the increase in the anodic currents upon application of the anodic potential up to points where

the currents level off in acidic solutions in Figure 4[30]. The leveling off in the current was attributed to the formation of a protective non-conducting WO_3(s) previously. The rate-determining step for the W anodic reaction in acidic solutions was reported to be the chemical dissolution of WO_3(s)[1,2,6−14,18,19,24,26,30], the overall formation of which can be expressed as in Equation 5:

$$W(s) + 3H_2O = WO_3(s) + 6H^+ + 6e^- \tag{5}$$

Therefore, the pH dependence of the steady-state anodic currents in acidic solutions in Figure 6 can be assumed to be the reflection of the pH-dependent chemical dissolution behavior of WO_3(s).

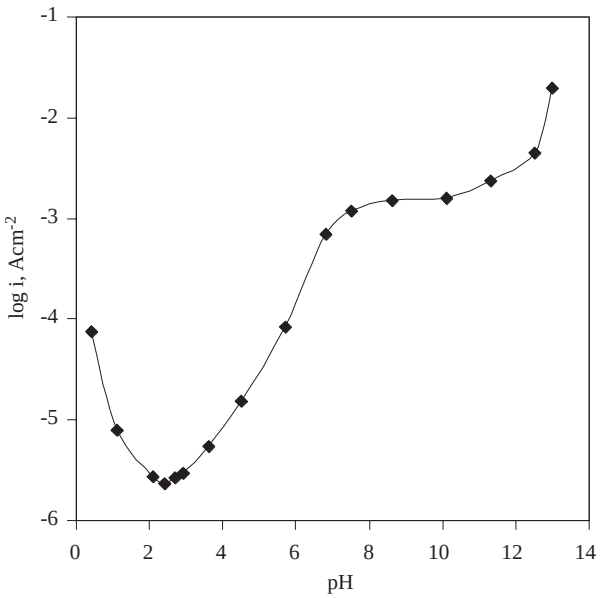

Figure 6. The pH dependence of the steady-state anodic currents at 1V.

The pH dependent chemical dissolution characteristics of the oxides are well-known[33−35]. In the absence of externally added ligands, dissolution is promoted either by H^+ or OH^-, resulting in a minimum in the dissolution rate vs. pH curve at the point of zero charge (pzc) of the corresponding oxide[33−35]. The surface concentration of the protonated (H^+ adsorbed) and deprotonated (OH^- adsorbed) sites are equal at the pzc and dissolution is lowest at this pH level because of the relatively low concentrations of these surface sites. At the pzc, the dissolution is assisted mainly by water molecules. The shape of the steady-state anodic current curve in Figure 6 in acidic solutions is consistent with the general scheme outlined above.

Below pH 2.5, which can be identified as the pzc of WO_3(s), the steady-state current increases as pH decreases in Figure 6 (also in Figures 4 and 5a). Therefore, the dissolution process must be H^+-assisted in this pH range. Although they are not present in the stability diagrams in Figures 1 and 2, the species WO_2^{2+}(aq) and WO_2OH^+(aq) were identified by spectrophotometric methods in very acidic solutions as W dissolution products[36,37]. The chemical dissolution behavior of WO_3(s) (the rate determining step in the W anodic reaction), therefore, can be assumed as in the following consecutive reactions in very acidic solutions[30]:

$$WO_3(s) + H^+ \rightarrow WO_2OH^+(aq) \tag{6}$$

$$WO_2OH^+(aq) + H^+ = WO_2^{2+}(aq) + H_2O \quad (7)$$

Around pH 2.5 (i.e., the pzc), the pH dependence of the steady-state current disappears in Figure 6. Therefore, as noted previously, the dissolution of WO_3(s) must be mainly promoted by the direct attack of water molecules in the neighborhood of this particular pH[30]:

$$WO_3(s) + H_2O \rightarrow WO_3.H_2O(s) = H_2WO_4(aq) \quad (8)$$

The presence of $WO_3.H_2O$(s) in acidic solutions (pH 1.6 in H_2SO_4) was evidenced by in-situ surface enhanced Raman spectroscopy[24].

As pH increases above pH 2.5, the pH dependence of the current commences again in Figure 6. The steady-state anodic current in this case, however, increases as pH increases to a pH value of 7. In this pH range (2.5–7), the dissolution of WO_3(s) is dominated by OH^--assistance as in Equation 9[30]:

$$WO_3(s) + OH^- \rightarrow WO_4^{2-}(aq) + H^+ \quad (9)$$

In summary, if the oxide formation reaction is expressed as in Equation 5, the overall W anodic reaction in acidic solutions is controlled by Equation 6 in a very acidic regime (pH $<$ 2.5), by Equation 8 at the pzc (pH 2.5), and by Equation 9 in a weakly acidic regime (2.5 $<$ pH $<$ 7).

The pH dependence of the steady-state current disappears in the pH range 7 to 10.5 in Figure 6. The metastable Eh-pH diagram in Figure 2 shows that the H_2WO_4(s) stability region extends up to pH 6. The kinetics (experimental results in Figure 6) suggest, however, that H_2WO_4(s) is present on W up to pH 10.5. Armstrong et al.[5] also observed this pH independent current region, and they concluded that anodic current is controlled by the following reaction:

$$H_2WO_4(s) \rightarrow H_2WO_4(aq) = WO_4^{2-}(aq) + 2H^+ \quad (10)$$

In the pH range 7 to 10.5, the protective oxide layer WO_3(s) must become highly hydrated ($WO_3.H_2O$(s)) and then solubilized as in the form in Equation 10.

As shown in Figure 6, above pH 10.5 the pH dependence of the steady-state current appears once again. Since the dissolution rate of W-oxides is quite high in basic solutions[3,4,8,10,17], the chemical dissolution of them cannot be the rate-determining step in the W anodic reaction. The open circuit potential was previously said to be controlled by Reaction 2 in basic solutions. This reaction must also be the rate determining step in the further anodizing of W in strongly basic solutions[8,30]. Reactions 3 and 4 take place right after Reaction 2 at a relatively high rate[8,30]. The limiting current at pH 13 in Figure 4 results from the slow diffusion of OH^- ions from the bulk solution to the electrode surface[30].

Conclusions

The anodic reaction characteristics of tungsten (W) were examined in a very broad pH range (0.4 to 13) in H_3PO_4-K_2SO_4-H_2SO_4/KOH solutions with an ionic strength of 2M. The open circuit potential of W shifted to less noble potential values with a constant slope of 58 mV/pH as pH increased. Dissolution was lowest at pH 2.5, which was identified as the point of zero charge of WO_3(s) formed on the metallic W in aqueous solution. At this particular pH the main dissolution pathway for the oxide was H_2O-assisted dissolution.

The oxide dissolution below pH 2.5 was H^+-assisted. In the pH range $2.5 < pH < 7$, however, OH^--assisted dissolution was observed. The pH independent current in the pH range 7 to 10.5 was attributed to the pH independent dissolution of the hydrated oxide phase. Above pH 10.5, the chemical dissolution of WO_3(s) was not the rate-determining step anymore, and the anodic currents were assumed to be controlled by the slow diffusion of OH^- ions.

Acknowledgment

This work was supported by Osmangazi University Research Fund (No: 2001/14).

References

1. I.A. Ammar and R. Salim, **Corros. Sci.**, **11**, 591-09 (1971).
2. J.W. Johnson and C.L. Wu, **J. Electrochem. Soc.**, **118**, 1909-12 (1971).
3. T. Heumann and N. Stolica, **Electrochim. Acta**, **16**, 643-51 (1971).
4. T. Heumann and N. Stolica, **Electrochim. Acta**, **16**, 1635-46 (1971).
5. R.D. Armstrong, K. Edmonson and R.E. Firman, **J. Electroanal. Chem.**, **40**, 19-29 (1972).
6. M.R. Arora and R. Kelly, **Electrochim. Acta**, **19-25**, 413 (1974).
7. A. Di Paola, F. Di Quarto, and G. Serravalle, **J. Less–Common Metals**, **42**, 315-24 (1975).
8. G.S. Kelsey, **J. Electrochem. Soc.**, **124**, 814-19 (1977).
9. A. Di Paola, F. Di Quarto, and C. Sunseri, **J. Electrochem. Soc.**, **125**, 1344-50 (1978).
10. A.D. Davydov, V.S. Krylov, and G.R. Engelgardt, **Elektrokhimiya**, **16**, 192-96 (1980).
11. M.S. El-Basiouny, S.A. Hassan, and M.M. Hefny, **Corros. Sci.**, **20**, 909-17 (1980).
12. A. Di Paola, F. Di Quarto, and C. Sunseri, **Corros. Sci.**, **20**, 1067-78 (1980).
13. F. Di Quarto, A. Di Paola, and C. Sunseri, **J. Electrochem. Soc.**, **127**, 1016-21 (1980).
14. F. Di Quarto, A. Di Paola, and C. Sunseri, **Electrochim. Acta**, **26**, 1177-84 (1981).
15. K. Osseo-Asare, **Metall. Trans. B**, **13**, 555-63 (1982).
16. **Tungsten Supplement A7**, Gmelin Handbook of Inorganic Chemistry, 8^{th} ed., 86-132, Springer-Verlag, Berlin (1987).
17. P.I. Ortiz, M.L. Teijelo, and M.C. Giordano, **J. Electroanal. Chem.**, **243**, 379-91 (1988).
18. A.S. Mogoda, M.M. Hefny, and G. A. El-Mahdy, **Corrosion**, **46**, 210-14 (1990).
19. A. Goussens and D.D. Macdonald, **J. Electroanal. Chem.**, **352**, 65-81 (1993).
20. E.A. Kneer, C. Raghunath, S. Raghavan, and J.S. Jeon, **J. Electrochem. Soc.**, **143**, 4095-4100 (1996).
21. A.D. Davydov, V.S. Shaldaev, A.N. Malofeeva, and I.V. Savotion, **J. Appl. Electrochem.**, **27**, 351-54 (1997).
22. J.M. Steigerwald, S.P. Murarka, and R.J. Gutmann, "**Chemical Mechanical Planarization of Microelectronic Materials**", 181-206, Wiley, New York (1997).

23. E.A. Kneer, C. Raghunath, V. Mathew, S. Raghavan, and J. S. Jeon, **J. Electrochem. Soc.**, **144**, 3041-49 (1997).
24. R.S. Lillard, G.S. Kanner, and D.P. Butt, **J. Electrochem. Soc.**, **145**, 2718-25 (1998).
25. D.J. Stein, D. Hetherington, T. Guilinger, and J.L. Cecchi, **J. Electrochem. Soc.**, **145**, 3190-96 (1998).
26. D.D. Macdonald, E. Sikora and J. Sikora, **Electrochim. Acta**, **43**, 2851-61 (1998).
27. D.J. Stein, D. Hetherington, and J.L. Cecchi, **J. Electrochem. Soc.**, **146**, 376-81 (1999).
28. J. Sikora, E. Sikora, and D.D. Macdonald., **Electrochim. Acta**, **45**, 1875-83 (2000).
29. A.D. Davydov, A.P. Grigin, U.S. Shaldaev, and A.N. Malofeeva, **J. Electrochem. Soc.**, **149**, E6-E11 (2002).
30. M. Anik and K. Osseo-Asare, **J. Electrochem. Soc., 149,** B224-B233 (2002).
31. W.J. Plieth, "**Nitrogen**" in Encyclopedia of Electrochemistry of the Elements, Vol. 8, ed. A.J. Bard, pp. 321-479, Marcel Dekker, New York (1978).
32. K. Osseo-Asare and T.H. Brown, Hydrometallurgy, 4, 217 (1979).
33. J.W. Diggle, "**Oxides and Oxide Films**", **Vol. 1**, 1-48, Marcel Dekker, New York (1972).
34. W. Stumm, "**Chemistry of the Solid-Water Interface"**, 64-85, Wiley, New York (1992).
35. M.A. Blesa, P.J. Morando, and A.E. Regazzoni, "**Chemical Dissolution of Metal Oxides"**, 121-186, CRC Press, Boca Raton (1994).
36. V.A. Nazarenko and E.N. Poluektova, **Russ. J. Inorg. Chem.**, **14**, 105-08 (1969).
37. V.A. Nazarenko and E.N. Poluektova, **Russ. J. Inorg. Chem.**, **22**, 551-54 (1977).